

Structures of the Common Cyclodextrins and Their Larger Analogues—Beyond the Doughnut

Wolfram Saenger,^{*} Joël Jacob, Katrin Gessler, Thomas Steiner, Daniel Hoffmann,[†] Haruyo Sanbe,[‡] Kyoko Koizumi,[‡] Steven M. Smith,[§] and Takeshi Takaha^{||}

Institut für Kristallographie, Freie Universität Berlin, Takustrasse 6, D-14195 Berlin, FRG, GMD-SCAI, Schloss Birlinghoven, D-53754 Sankt Augustin, FRG, School of Pharmaceutical Sciences, Mukogawa Women's University, 11-68 Koshien, Kyuban-cho, Nishinomiya, Hyogo 663, Japan, Institute of Cell and Molecular Biology, University of Edinburgh, The King's Buildings, Mayfield Road, Edinburgh EH9 3JH, United Kingdom, and Biochemical Research Laboratory, Ezaki Glico Co., Ltd., 4-6-5 Utajima, Nishiyodogawa, Osaka 555, Japan

Received November 4, 1997 (Revised Manuscript Received April 9, 1998)

Contents

I. Introduction: General Description of Cycloamyloses	1787
II. Structural Features of Cyclodextrin Molecules	1790
1. The Glucose Is a "Rigid" Unit	1790
2. The Macrocyclic Geometry Is Well-Defined in CA6 to CA9	1790
3. The Torsion Angle Index	1791
4. A Ring of Intramolecular O2(<i>n</i>)...O3(<i>n</i> −1) Hydrogen Bonds	1792
5. Glucosyl Torsion Angles ϕ and ψ Are Rather Constant	1792
III. Two Types of Crystal Structures: Channels and Cages	1792
1. Channel-Type Structures	1793
2. Cage-Type Structures in Herringbone and Brick Motifs	1793
3. What Are the Conditions for Formation of Channel- or Cage-Type Crystal Structures?	1794
IV. Cycloamyloses Have Many O—H...O and C—H...O Hydrogen Bonds	1794
1. Intramolecular, Interglucose O2(<i>n</i>)...O3(<i>n</i> −1) Hydrogen Bonding as Primary Source of CA Structural Stability	1794
2. Cooperative Networks Formed by O—H...O Hydrogen Bonds	1794
3. Flip-Flop Hydrogen-Bond Disorder in CA7	1795
4. C—H...O Hydrogen Bonding Occurs if There Is a Lack of O—H Donors	1795
V. Diffusion of Water Molecules in the Crystal Lattice of Ca7·12H ₂ O.	1796
VI. Ca9 Is the Intermediate between Smaller and Larger Cycloamyloses	1796
VII. Strain-Induced Flips of Glucoses and Kinks in Ca10 and Ca14	1797
1. ¹³ C NMR Spectra Indicate Different Structures	1797
2. CA10 and CA14 Are Not Doughnut-Shaped	1797
3. "Band Flips and Kinks as New Structural Features in CA Containing More than Nine Glucoses	1798
4. Band Flips Must Occur Due to Conformational Strain	1799
5. Extension of the Structure of CA10 and CA14 to Very Large CA—A Plausible Model	1799

6. CA10 and CA14 in Solution—Do They Form Inclusion Complexes?	1800
VIII. A Glimpse at the Structure of CA26—Déjà Vu Cyclodextrin and Band Flips: The V-Amylose Helix	1800
IX. Outlook	1801
X. Acknowledgments	1801
XI. References	1801

I. Introduction: General Description of Cycloamyloses

If the amylose fraction of starch is degraded by glucosyltransferases, one or several turns of the amylose helix are hydrolyzed off and their ends are joined together, thereby producing cyclic oligosaccharides called cyclodextrins (CDs) or cycloamyloses (CAs). Since these enzymes are not very specific, a family of macrocycles with different numbers of glucose units are produced.^{1,2} The most abundant are α -, β -, and γ -cyclodextrin with six, seven, and eight glucoses respectively; they are also called, and in this article used throughout, cyclohexa-, cyclohepta-, and cyclooctaamylose or CA6, CA7, CA8. These doughnut-shaped molecules have been investigated with the use of spectroscopic, kinetic, and crystallographic methods,^{1–5} and there is only one X-ray crystal structure analysis of the larger δ -CD or CA9.⁶ Beyond that, the crystal structures of two larger members of the cyclodextrins have recently been published, namely that with 10 glucoses (ϵ -CD or CA10)^{7,8} and that with 14 glucoses in the ring (ι -CD or CA14),⁷ and the crystal structure of an even larger cyclodextrin with 26 glucoses (CA26) has been obtained.⁹ Whereas larger cyclodextrins with more than 100 glucoses in the ring and beyond have been prepared by the action of disproportionating enzyme on amylose,¹⁰ smaller molecules would be sterically strained

^{*} Corresponding author, Institut für Kristallographie, Freie Universität Berlin, Takustr. 6, D-14195 Berlin, FRG. Telephone: +49-30-838-3412. Fax: +49-30-838-6702. E-mail: saenger@chemie.fu-berlin.de.

[†] GMD-SCAI, Schloss Birlinghoven.

[‡] Mukogawa Women's University.

[§] University of Edinburgh.

^{||} Ezaki Glico Co., Ltd.



Wolfram Saenger graduated from Technische Hochschule Darmstadt in Chemistry and received his Ph.D (1965). After a postdoctoral stay at Harvard University with Professor J. Z. Gougoutas, he joined the Max-Planck-Institut für experimentelle Medizin in Göttingen where he set up an independent research group working on X-ray crystal structure analysis of oligosaccharides, proteins, nucleic acids. In 1972, he received his Habilitation from the Universität Göttingen, and since 1981, he holds the chair for crystallography at Freie Universität Berlin. In 1987, he received the Leibniz Award and in 1988 the Humboldt Award. Besides structural biology, current interests are in hydrogen bonding and protein aggregation leading to crystallization.



Katrin Gessler received her degree in Chemistry from the University Leipzig doing biochemical investigations on cyclodextrin-producing enzymes and crystal structure analysis on cyclodextrin inclusion complexes. She then worked at the Institute of Crystallography of the Free University Berlin for her Ph.D. under supervision of Professor W. Saenger, titled "The crystal structure of β -D-cellobiose, the new model for cellulose II and hydrogen bonding systems". Since 1995, she has been working in a postdoctoral position on crystal structure investigations of biological carbohydrate polymers. Her interests focus on the structures of cyclodextrins with several degrees of polymerization and their inclusion complexes.



Joël Jacob received his degree in chemistry from the University of Liège (Belgium) in 1995 after working one year in the group of Professor J. van der Maas at the University of Utrecht (The Netherlands). In his master thesis, he investigated weak hydrogen bonds using vibrational spectroscopy. Since 1995, he has been a Ph.D. student under the direction of Professor W. Saenger and Dr. K. Gessler at the Free University of Berlin, Institute of Crystallography. His current research interests include the structural investigations of large cyclodextrins using X-ray crystallography and spectroscopic techniques.



Thomas Steiner graduated 1986 in experimental physics at the Technische Universität Graz (Austria). He obtained his Ph.D. at the Freie Universität Berlin in 1990, where he worked with Professor Wolfram Saenger doing neutron scattering studies of cyclodextrin complexes. Following a postdoctoral period in the same laboratory, he started independent research work on weak hydrogen bonding, isotropic intermolecular interactions, structure correlation, and crystal engineering. In 1998, he is a guest researcher at the Department of Structural Biology of the Weizmann Institute of Science, Israel.

and are therefore not produced by the glucosyltransferase enzymes.

The chemical structure of CA7 is presented in Figure 1. It immediately suggests that this molecule and the related CA6 and CA8 are able to accommodate small guest molecules that fit spatially within the cavities formed by the annular structures. This particular feature distinguishes CA from most other host molecules which per se are unable to form inclusion complexes and require crystallization into a lattice in order to provide a matrix with suitable cavities.

As in amylose, the glucose units in the CAs are linked by $\alpha(1-4)$ bonds and adopt the 4C_1 chair conformation. They may be considered as fairly rigid building blocks, the only conformational freedom of

the macrocycle residing in rotation of the C6–O6 groups and (limited) rotational movements about the glucosidic link C1(n)–O4($n-1$)–C4($n-1$). Since all glucoses are aligned in register (in cis) with the secondary O2 and O3 hydroxyls on one side connected by O2(n)...O3($n-1$) hydrogen bonds, and the primary O6 hydroxyls on the other side, the smaller CA6 to CA8 have the overall shape of a hollow, truncated cone with the wide side occupied by O2 and O3 and the narrow side by O6.

One of the most important features of CA concerns the distribution of hydrophilic and hydrophobic groups. Because the hydrophilic hydroxyl groups occupy both rims of the cone, they render the CAs soluble in water. The inside of the cavity, however, is hydrophobic in character since it is covered by C3–H, C5–



Daniel Hoffmann received his degree in Physics/Astronomy from the University of Heidelberg with a thesis at the Max-Planck-Institute for Medical Research in Heidelberg under the direction of Ulrich Haeberlen. He earned his Ph.D. working with Ernst-Walter Knapp at the Institute of Crystallography/Department of Chemistry, Free University of Berlin. In 1996, he joined the group of Thomas Lengauer at the German National Research Center for Information Technology. Currently, his interests include the modeling of biomolecular systems and teaching science.



Haruyo Sanbe received her bachelor's degree of pharmaceutical sciences from Mukogawa Women's University in 1996. She is currently pursuing a master's degree of pharmaceutical sciences in the same university, where she is working with Professor Kyoko Koizumi. Her current studies focus on the isolation and characterization of cyclic α -1,4-glucans and their enzymic synthesis.

H, and C6–H₂ hydrogens and by the ether-like oxygens O4. Consequently, the cavities provide a hydrophobic matrix in aqueous solution, which led to the term “microheterogeneous environment”.¹²

The unique structural properties of the CA cavity explain some of the unusual features of these molecules. They form inclusion complexes rather non-specifically with a wide variety of guest molecules, the only obvious requirement being that the guest molecule must fit into the cavity, even if only partially. Consequently, it is not surprising to find that noble gases, paraffins, alcohols, carboxylic acids, aromatic dyes, benzene derivatives, salts, and water are included, just to name a few of a long list of potential guest substances.^{1–3,12–14} The most interesting inclusion complexes of the CAs are of course those which are of importance to the chemical, pharmaceutical or food industry.¹⁴ As they will be the topic of other articles in this issue, they are not treated here further. CAs are, however, not only of practical value but they have been studied in detail because they are prototypes for the investigation of

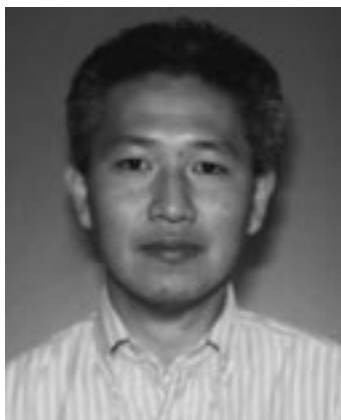


Kyoko Koizumi received her bachelor's, master's, and doctor's degrees of pharmaceutical sciences from Osaka University. She worked for five years and seven months at the faculty of pharmaceutical sciences, Osaka University, but also worked as a research associate for two years and three months with Professor L. Wolfrom at the department of chemistry, The Ohio State University. She moved to the school of pharmaceutical sciences, Mukogawa Women's University as an associate professor in 1966 and has been a professor of analytical chemistry at the same university since 1976. Her current research interests are separation analysis of carbohydrates, especially oligo- and polysaccharides, and enzymatic synthesis of novel heterobranch cyclodextrins and their inclusion reactions.



Steven M. Smith received his M.A. from Indiana University, under the supervision of Professor Carlos Miller, working on cytokinin action in plants. He then studies for a Ph.D. with Professor John Ellis in the Department of Biological Sciences at the University of Warwick, UK, working on protein import into chloroplasts. Between 1980 and 1982 he carried out postdoctoral research in the Commonwealth Scientific and Industrial Research Organisation, Canberra, Australia, investigating the expression of genes encoding chloroplast proteins. Since 1983, he has been a faculty member at the University of Edinburgh. His current research involves several aspects of carbohydrate metabolism and function in plants, including sugar sensing and transduction mechanisms which control gene expression and enzyme synthesis. Recently work on the characterization and manipulation of enzymes of starch metabolism has led to investigations of the function and applications of glucanotransferases.

noncovalent interactions between different molecules which are so ubiquitous in all aspects of molecular recognition in chemistry, supramolecular chemistry, and biology.^{12,15} These interactions are mainly of the van der Waals or hydrogen bonding type and can be studied with the CAs using crystallographic methods.^{3–5,13} Crystals of CA inclusion complexes generally permit data collection to high resolution (<1 Å) and grow large enough for neutron diffraction to be carried out, thereby providing a rich source for studies on hydrogen bonding where the accurate



Takeshi Takaha received his bachelor's degree in engineering from Osaka University and has been working for Ezaki Glico Co. Ltd. (Osaka, Japan) since 1983. Between 1991 and 1993 he carried out research on potato glucanotransferase under the direction of Dr. Steven M. Smith in Edinburgh and after completing this research in Osaka was awarded his Ph.D. by the University of Edinburgh in 1997. His current research interests include studies of the enzymes involved in the synthesis and degradation of starch (glycogen) and utilization of such enzymes for the production of useful carbohydrates.

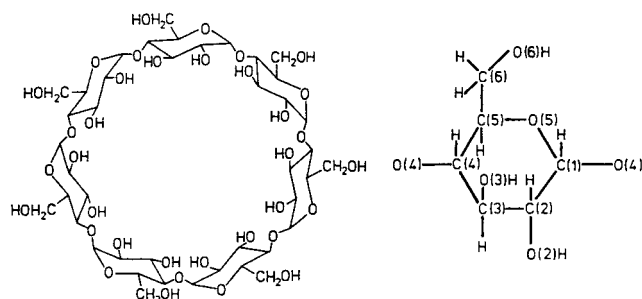


Figure 1. (left) Chemical structure of CA7 (β -cyclodextrin); according to IUPAC rules,¹¹ numbering of glucoses 1 to 7 is counterclockwise; and (right) atom numbering scheme of a glucose unit.

positions of hydrogen atoms must be known.¹⁶ In addition to crystallographic studies, the inclusion process of the CAs has been investigated in terms of kinetics and thermodynamics using spectroscopic methods.³

There have been many attempts to modify the glucose units in the CAs by chemical methods.¹⁷ The main interest in these modifications was to improve the inclusion properties of the CAs for industrial applications by simple extension of the length of the cone with alkyl groups. In other, more sophisticated approaches, functional groups were attached to one, some, or all of the hydroxyl groups to further enhance the naturally observed enzyme-like activity that the CAs exhibit due to their inclusion properties and the high density of hydroxyl groups on their rims. In a wide variety of studies these model enzymes have been characterized in terms of inclusion and catalytic properties.^{14,15}

II. Structural Features of Cyclodextrin Molecules

1. The Glucose Is a "Rigid" Unit

By and large, the overall shapes and the 4C_1 chair conformation of individual glucose units in all CAs so far investigated are comparable, no matter what

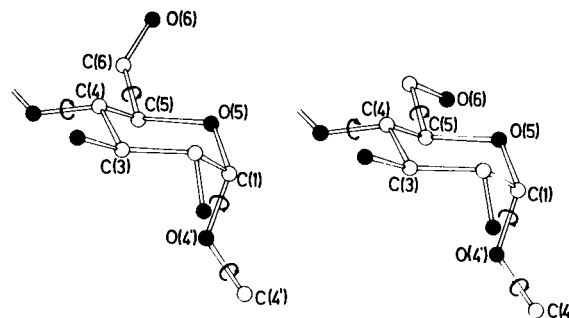


Figure 2. Glucose 4C_1 chair conformation with O6–H in (–)gauche (left) and (+)gauche (right) orientations. Bonds about which rotations are likely to occur in cycloamyloses are indicated by circles.⁴

guest is included within the cavity.^{4,5} Moreover, the endocyclic torsion angles in the glucose rings are confined to (+)- or (–)gauche within a narrow range, as indicated by comparable values of Cremer–Pople puckering parameters,¹⁸ suggesting that the glucose can be considered as a fairly "rigid" building block (Table 1). This does not hold strictly for fully methylated CA7 where, in inclusion complexes, severe distortions of the 4C_1 chair form were observed¹⁹ and in the monohydrate, one glucose even adopts the inverted 1C_4 form.²⁰

By contrast, the primary O6–H hydroxyl group can rotate about the C5–C6 bond (Figure 2). In principle, three staggered orientations (+)gauche, (–)gauche, and trans can be adopted by the O5–C5–C6–O6 torsion angle, yet only the first two have actually been observed in CAs; trans has not been found thus far. A reason for this behavior could be that in the trans orientation, adverse steric interactions might occur between O6–H and atoms of the adjacent glucose unit in the ring. In addition, the gauche effect,^{21,22} operative in O–C–C–O systems, should also destabilize the trans arrangement.

The two gauche conformers are not equally common, the (–)gauche form with O6–H pointing "away" from the center of the cavity (Figure 2) being largely preferred. The (+)gauche orientation with O6–H "toward" the cavity is only found in crystal structures if certain packing requirements are met or if a hydrogen bond is formed with an included guest molecule.

2. The Macrocyclic Geometry Is Well-Defined in CA6 to CA9

Some remarkable features are observed concerning the overall shape of the CAs. Above all, the O4 atoms defining the macrocyclic hexa-, hepta-, octagons are virtually coplanar, with less than 0.25 Å deviation from the common mean plane, but larger deviations are observed for the nonagon in CA9.⁶ The O4(*n*)...O4(*n*–1) distances forming the edges of the macrocycles are more or less constant within each member of the CA family; they increase, however, from CA6 to CA8 because the glucose unit has to adjust to the respective radius of the CAs. For CA8 and larger ring sizes they are roughly constant, ~4.5 Å (Table 1).

In line with these observations are distributions of O4(*n*)...O4(*n*–1)...O4(*n*–2) angles, which are around

Table 1. Some Physical Characteristics of CA6, CA7, CA8, CA9, CA10, and CA14 and Structural Parameters of the Hydrates

		CA6	CA7	CA8	CA9	CA10	CA14
number of glucose units		6	7	8	9	10	14
molecular weight		972	1135	1297	1459	1621	2270
solubility in water g/100 mL at room temperature		14.5	1.85	23.2			
$[\alpha]^{1.4}$		150 ± 5	162.5 ± 5	177.4 ± 5			
cavity diameter, Å		4.7–5.3	6.0–6.5	7.5–8.3			
height of cone, Å		7.9 ± 1	7.9 ± 1	7.9 ± 1			
volume of cavity, Å ³		174	262	472			
pK by potentiometry, 25 °C		12.33	12.20	12.08			
partial molar volumes in solution, (mL mol ⁻¹)		611.4	703.8	801.2			
Structural Parameters of the Hydrates ^{a–f}							
torsion angles ϕ^g	av	109.2 ^a	109.8 ^b	108.9 ^c	112.1 ^d	99.4	103.4
	min.	102.0 ^a	102.3 ^b	103.6 ^c	88.4 ^d	94.1 ^e	96.6 ^f
	max.	114.9 ^a	118.6 ^b	123.2 ^c	141.2 ^d	102.1 ^e	110.2 ^f
torsion angles ψ^g	av	128.8 ^a	127.6 ^b	127.1 ^c	124.7 ^d	106.1	112.6
	min.	115.1 ^a	114.2 ^b	111.9 ^c	97.6 ^d	96.3 ^e	103.6 ^f
	max.	148.7 ^a	140.4 ^b	138.5 ^c	144.5 ^d	122.0 ^e	135.2 ^f
angles O4(<i>n</i>)...O4(<i>n</i> –1)...O4(<i>n</i> –2)	av	119.9	128.3	134.9	136.6	138.2	138.2
	min.	116.9	125.2	133.5	125.7	126.7	131.6
	max.	122.3	132.5	136.9	149.9	145.9	142.5
distances O4(<i>n</i>)...O4(<i>n</i> –1)	av	4.235	4.385	4.502	4.489	4.488	4.54
	min.	4.158	4.267	4.433	4.262	4.36	4.45
	max.	4.298	4.499	4.592	4.734	4.63	4.61
distances O2(<i>n</i>)...O3(<i>n</i> –1)	av	2.981	2.884	2.823	2.906	2.927	2.83
	min.	2.902	2.801	2.765	2.741	2.85 ^e	2.76 ^f
	max.	3.150	2.978	2.911	3.234	3.01 ^e	2.90 ^f

^a In the “round” α -cyclodextrin·7.52H₂O, ref 44. ^b In β -cyclodextrin·11H₂O, ref 51. ^c In γ -cyclodextrin·14H₂O, see ref 38. ^d In δ -cyclodextrin·13.75H₂O, ref 6. ^e In CA10·H₂O, only the three values without flip and kink, ref 7. ^f In CA14·H₂O, only the five values without flip and kink, ref 7. ^g For definition see ref 11.

120° in CA6, 128° in CA7, and 135° in CA8, with variations within $\pm 5^\circ$. Exceptions from these rather constant macrocyclic data are only observed for the smallest member, CA6. In the hexahydrate of CA6, the macrocycle is somewhat collapsed due to the insertion and tight fit of the small H₂O in the cavity (see also section IV), and in the complexes formed between CA6 and para-disubstituted benzene derivatives, the diameter of the benzene ring is wider than the cavity so that the CA6 macrocycle is elliptically distorted.²³ The data given in Table 1 and in Figure 3 describe the average geometry of the macrocycles

and of the glucose unit; they are more or less constant and not or only slightly modified by inclusion of guest molecules. This means that upon complex formation, the guest has little or no influence on the conformations of the glucoses but may slightly distort the macrocycle of the enclosing CA.

3. The Torsion Angle Index

French and co-workers noted a correlation between the O4(*n*)...O4(*n*–1) distance and a certain combination of endocyclic torsion angles in several pyranoses.^{24,25} This interrelation can also be found for CA6 complexes in different crystal forms, for which the diagram shown in Figure 4 is obtained.²⁶ There is an obvious, almost linear correlation observed for brick-type cage structures (see section III) formed by CA6 and the above-mentioned para-disubstituted benzene derivatives, indicating that the distortions of CA6 as expressed by O4(*n*)...O4(*n*–1) variations of about 0.5 Å are also reflected in changes of endocyclic torsion angles. This correlation for the para-disubstituted benzene derivatives extends over the whole plot in Figure 4, whereas data for CA6 inclusion compounds crystallizing in cage-type structures with herringbone arrangement (see section III) and with channel-type structures are more narrowly clustered in the center of the diagram, showing that the CA6 molecules are less distorted if the guest molecules are not of the para-disubstituted benzene type. As to CA7 and CA8, the conformations of the macrocycles and of the individual glucose units are only marginally influenced by the guest molecules so that the torsion angle index is confined to the center of the diagram.

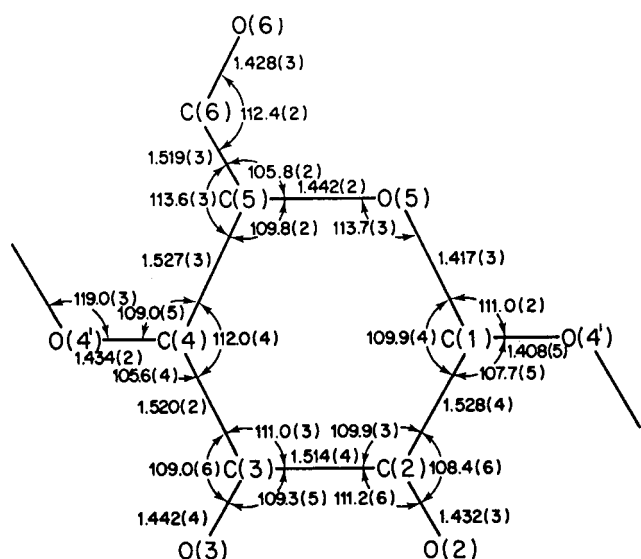


Figure 3. Average geometry for the glucose unit in α -cyclodextrin-methanol-5 H₂O. Standard deviations in parentheses.²³

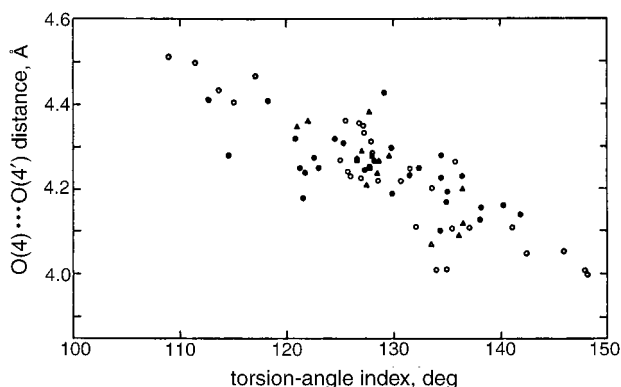


Figure 4. Correlation of $O(4)(n) \cdots O(4)(n-1)$ distance with torsion angle index in α -cyclodextrin complexes with para-substituted benzenes (O, brick-type cage motif); complexes with herringbone cage motif (●) and with channel-type motif (Δ). Torsion angle index defined as:^{19,20} $|\phi \text{ C1-C2}| + |\phi \text{ C2-Ce}| + |\phi \text{ C5-O5}| + |\phi \text{ O5-C1}| - |\phi \text{ C3-C4}| - |\phi \text{ C4-C5}|$ with $\phi \text{ C1-C2}$ torsion angle O5-C1-C2-C3 etc. From ref 26.

4. A Ring of Intramolecular $O(2)(n) \cdots O(3)(n-1)$ Hydrogen Bonds

The remarkable structural rigidity of the CA macrocycle appears to be primarily due to a ring of hydrogen bonds. It is found in all the CA crystal structures investigated so far and formed intramolecularly between $O(2)\text{-H}$ and $O(3)\text{-H}$ hydroxyl groups of adjacent glucose units which are oriented cis. The average $O(2)(n) \cdots O(3)(n-1)$ distance is not constant for all CAs but decreases from CA6 (2.98 Å) through CA7 (2.88 Å) to CA8 (2.82 Å), indicating that hydrogen bonds become increasingly stronger going from CA6 to CA8 (Table 1). This statement is corroborated by measurements of hydrogen/deuterium exchange in aqueous solution which is rather slow per se in CA and indicative of strong hydrogen bonding.^{27,28} As established by H/D exchange rates, hydrogen bonding is stronger for CA7 than for CA6, in agreement with the average $O(2)(n) \cdots O(3)(n-1)$ distances and their variations. Whereas the variations are small (~ 0.2 Å) for CA7 and CA8 (Table 1), they can be much larger in CA6 to the extent that $O(2)(n) \cdots O(3)(n-1)$ distances are > 3.5 Å and hydrogen bonds are broken. This is observed for $\text{CA6} \cdot 6\text{H}_2\text{O}$ where one glucose is rotated out of register with the other five (vide infra) and in the elliptically distorted CA6 in complexes with hydroquinone $\cdot 6\text{H}_2\text{O}$ ²⁹ and with benzaldehyde $\cdot 6\text{H}_2\text{O}$.³⁰

The $O(2)(n) \cdots O(3)(n-1)$ hydrogen bonds are special because they are the major components of three-center bonds, the minor components donating to the O4 atom linking the two respective glucose units³¹ (Figure 5). Although this should add only weakly to the overall stability of the CA macrocycle, it will contribute to its rigidity as it will strengthen the $O(2)(n) \cdots O(3)(n-1)$ hydrogen bonding interactions.

As to the $O(6)\text{-H}$ hydroxyl groups, they are frequently engaged in intraglucose hydrogen bonding of the type $O(6)\text{-H} \cdots O(5)$, and in most cases represent the minor component of three-center hydrogen bonding interactions; sometimes these interactions are

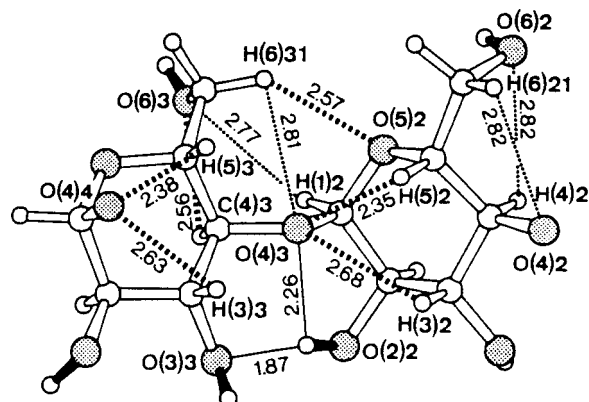


Figure 5. Detail of the crystal structure of β -cyclodextrin ethanol $\cdot 8\text{D}_2\text{O}$ determined by neutron diffraction at 15 K. Hydroxyl group $O(2)2$ donates a three-center hydrogen bond, with major component to $O(3)3$ ($\text{D} \cdots \text{O}$ at 1.87 Å) and minor component to $O(4)3$ ($\text{D} \cdots \text{O}$ at 2.26 Å). Filled covalent bonds represent O-D ; thick broken lines are $\text{C-H} \cdots \text{O}$ hydrogen bonds with $d_{\text{H} \cdots \text{O}} < 2.7$ Å; dotted lines with $2.7 \text{ Å} < d_{\text{H} \cdots \text{O}} < 3.0$ Å; thin lines are $\text{O-D} \cdots \text{O}$ bonds. Note systematic occurrence of $\text{C3-H} \cdots \text{O4}$, $\text{C5-H} \cdots \text{O4}$ and $\text{C6-H} \cdots \text{O4}$ interactions which stabilize the glucose conformation. Reprinted from ref 31. Copyright 1992 American Chemical Society.

mediated by water molecules $\text{O6} \cdots \text{W} \cdots \text{O5}$, where O6 and O5 again belong to the *same* glucose.⁴

5. Glucosyl Torsion Angles ϕ and ψ Are Rather Constant

The intramolecular $O(2)(n) \cdots O(3)(n-1)$ hydrogen bonds stabilize the macrocyclic conformation and the orientation of one glucose unit relative to its adjacent neighbors. This, on the other hand, limits the conformational space of torsion angles ϕ and ψ describing rotations about the glucosyl $\text{C1}(n)\text{-O4}(n-1)$ and $\text{O4}(n-1)\text{-C4}(n-1)$ bonds. In this paper, ϕ and ψ are defined as $\text{O5}(n)\text{-C1}(n)\text{-O4}(n-1)\text{-C4}(n-1)$ and $\text{C1}(n)\text{-O4}(n-1)\text{-C4}(n-1)\text{-C3}(n-1)$, respectively (see footnote Table 1 and ref 11). The average ϕ , ψ torsion angles are virtually identical for CA6 to CA8 and, in general, do not deviate markedly from the values given in Table 1 except for the unusual hexahydrate of CA6. Associated with the increased ring size, the larger CA9 displays some conformational instability relative to CA6 to CA8 with extreme values of ϕ , 88.5° to 141.2° and ψ 97.6° to 144.5° , respectively.⁶

III. Two Types of Crystal Structures: Channels and Cages

CAs are easily dissolved in water (Table 1) and crystallize with their cavities filled only by water molecules. For the crystallization of an inclusion complex of a CA, one has to add the guest molecule in manifold molar excess to form the complex because the dissociation constants are in the molar to minimolar range, indicating weak affinities. If CA6 to CA8 are crystallized either as hydrate or as inclusion complex, the molecules are arranged within the crystal lattice in one of two modes described as cage and channel structures according to the overall appearance of the formed cavities,³² see Figure 6.

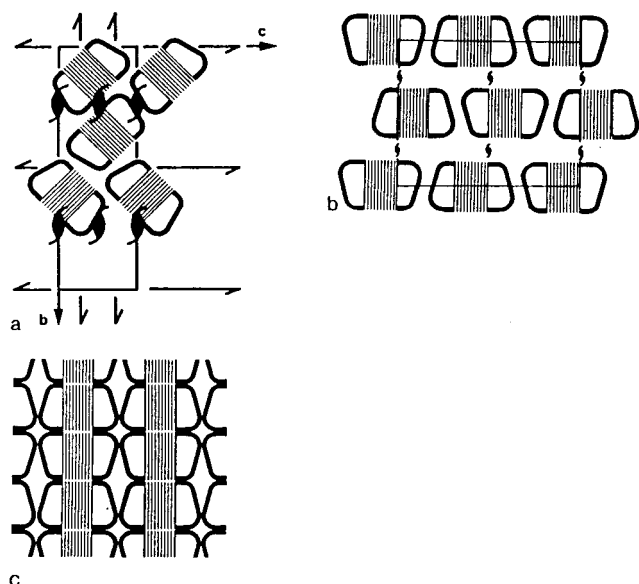


Figure 6. Schematic description of (a) herringbone, (b) brick-type, and (c) channel crystal structures formed by cyclodextrin inclusion complexes. Taken from refs 4 and 32.

1. Channel-Type Structures

In channel-type complexes, CA molecules are stacked on top of each other like coins in a roll, and the now linearly aligned cavities form "infinite" channels in which the guest molecules are embedded (Figure 6c). The stacks of CA are stabilized by hydrogen bonds either between O2–H/O3–H and O6–H sides producing head-to-tail patterns, or between O2–H/O3–H and O2–H/O3–H on one side and between O6–H and O6–H on the other side leading to head-to-head arrangement. In general, in one particular crystal structure only one type of stack is formed. In CA8 complexed with small organic molecules, however, a unique situation is encountered because head-to-tail and head-to-head orientations alternate within the same stack, with three stacked CA8 molecules forming the repeating unit along the stack axis, see Figure 7.

Another related packing motif is frequently observed with CA7 in which the stack consists of CA7 dimers hydrogen bonded with their O2–H/O3–H sides. They form basket-like units in which guest molecules are accommodated. The dimers are then stacked and interact with their O6–H sites to form the channel structure.

It goes without saying that the channels are not always straight, and frequently the individual CA molecules are tilted with respect to the channel axis. Only in cases where a crystallographic symmetry axis coincides with the channel axis the CA macrocycle is exactly perpendicular to the channel (symmetry) axis.

2. Cage-Type Structures in Herringbone and Brick Motifs

In crystal structures belonging to the cage type, the cavity of one CA molecule is blocked off on both sides by adjacent CAs, thereby leading to isolated cavities

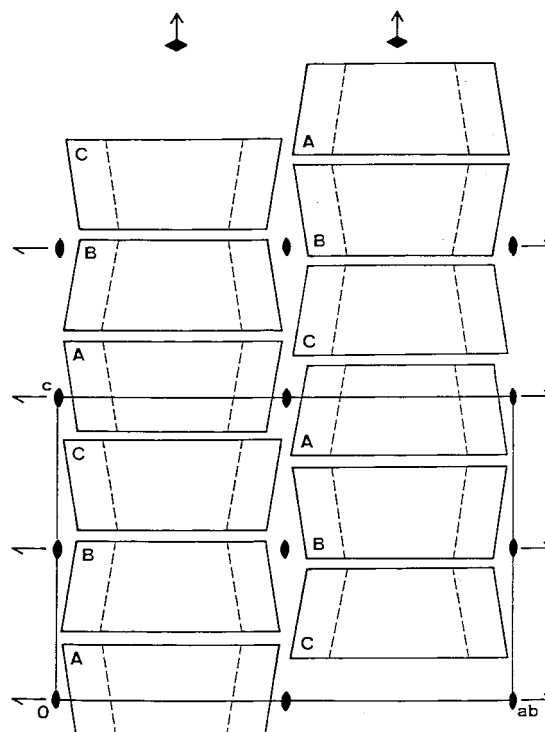


Figure 7. Schematic description of the crystal structure of γ -cyclodextrin (CA8) inclusion complexes other than water. The space group is $P4_212$, the positions of symmetry elements are indicated by respective symbols. There are $3 \times \frac{1}{4}$ molecules in the asymmetric unit, denoted A, B, and C. The intermolecular contacts are head-to-tail for A/B, tail-to-tail for B/C, and head-to-tail for C/A. Reprinted from ref 40.

in which the guest molecules are not in contact with each other.

With the cage-type structures, two different categories are encountered, depending on the packing of the CA molecules. In one, CAs are packed cross-wise in herringbone fashion, Figure 6a; this packing motif is observed for CA6 to CA9 if cocrystallized with water, and if CA6 is cocrystallized with krypton and with small molecules such as iodine, methanol, or propanol. As to CA7, the cage-type packing is observed with small alcohols, whereas complexes with larger alcohols and other guest molecules prefer the channel type. With CA8, cage-type packing is only observed with water, and all other guest molecules induce the channel form.³³

The other cage-type packing is observed when CA6 is complexed with para-disubstituted benzene derivatives³⁴ or with a dimethyl sulfoxide/methanol³⁵ mixture (Figure 6b). The obtained packing motif is reminiscent of bricks in a wall; the CA6 molecules are arranged in layers, and adjacent layers are laterally displaced so that the cavity of each CA6 is closed on both sides by molecules in adjacent layers. Besides CA6, this brick-type packing is also observed with CA7. It can form a different brick-type packing motif, in which dimer "baskets" are stabilized intermolecularly by hydrogen bonding between O2–H/O3–H sides and arranged in layers which are displaced laterally. In fact, this brick-type pattern can be considered as a variety of the channel motif in which every second unit is displaced with respect to

the channel axis so that the channel is disrupted and individual cages are produced. For the CA7 dimer, all kinds of different forms of this variety have been observed, from truly channel to truly brick-type packing.

3. What Are the Conditions for Formation of Channel- or Cage-Type Crystal Structures?

The answer is that we can predict the type of crystal packing only for CA6 with some degree of certainty. As discussed in an early survey of crystalline CA6 inclusion complexes,³⁶ small molecular guests form cages, whereas long molecular and ionic guests prefer channels. This behavior is especially obvious with carboxylic acids: CA6 complexes with acetic, propionic, and butyric acids crystallize in cages whereas valeric acid and higher analogues form channels—a clear and well-defined size selectivity.³⁶ A good example for a pair of molecular and ionic guests is acetic acid. Molecular acetic acid (the free acid) crystallizes as a complex with CA6 in a cage structure, contrasting with the inclusion complex of the salt, potassium acetate, which produces a channel structure. In the latter, acetate ions and water molecules are located within the channel and are disordered, and potassium ions are hydrated by water molecules and located in external interstices.³⁷

The situation for CA7 appears to be different, and prediction of channel or cage forming guests is not possible so far. In any case, the dodecahydrate as well as methanol, ethanol, and hydroiodide complexes of CA7 crystallize as cage-type complexes. 1-Propanol, which easily fits into the cavity, induces a change to the channel type for CA7, in contrast to CA6 which crystallizes in the cage type with this guest molecule. As for CA8, a herringbone cage-type complex has only been obtained for CA8·15.7H₂O,^{38,39} whereas other guest molecules, even the small methanol, induced the channel form.⁴⁰ It appears, therefore, that generalizations can be made only for CA8, and extrapolations to other CAs are not possible.^{32,36}

Is there any rationale for the preferred channel complex formation of CA7 and CA8? The channels formed by CA6 are mostly of the head-to-tail form and only in some complexes such as polyiodides formed by disordered triiodides, do head-to-head structures occur.⁴¹ By contrast, in most CA7 channel structures, the CA7 molecules are arranged head-to-head. In channel type structures formed by CA8, alternating head-to-head/head-to-tail distributions are found.^{33,40} It appears likely that, as proposed for the complexes formed between polyiodides and CA6, dimer formation with CA7 occurs already in aqueous solution with appropriate guests, the CA7 molecules being hydrogen bonded head-to-head via O2—H/O3—H hydroxyl groups. These “baskets” contain the guests and crystallize in linear aggregates to produce channels. Arguments for the “basket” hypothesis are the many channel-type structures exhibiting different molecular packing with variations extending to the brick-type motif.

IV. Cycloamyloses Have Many O—H···O and C—H···O Hydrogen Bonds

1. Intramolecular, Interglucose O2(*n*)···O3(*n*−1) Hydrogen Bonding as Primary Source of CA Structural Stability

As thermodynamic studies have indicated, CA6 is able to form four different hydrates when crystallized from water, three of which have been analyzed by X-ray methods.^{42–44} In one of them, the CA6 macrocycle adopts a “round” shape with all O2(*n*)···O3(*n*−1) hydrogen bonds formed; 2.57 water molecules are enclosed in the cavity and statistically distributed over four disordered sites.⁴⁴ In the other two complexes, all water molecules are fully ordered, but the CA6 macrocycle is partly collapsed by rotation of one glucose unit out of the alignment with the other five. This rotation leads to a “kink”-like discontinuity further discussed below (section VII.3), and disrupts two of the six interglucose O2(*n*)···O3(*n*−1) hydrogen bonds; it moves the O6—H of this rotated glucose closer to the center of the CA6 molecule so that a hydrogen bond to one of the included water molecules is formed. As a consequence, the volume of the cavity is reduced to provide a good fit for these water molecules; it is in hydrogen bonding contact with another water close to the O2—H/O3—H rim in the complex called form I.⁴² In form II,⁴³ this second water is replaced by the O6—H of an adjacent CA6, thus forming a self-complex.

This conformation of CA6, where one glucose is rotated out of register with the other five, has only been observed with water as guest molecule (see section II.4). If water is replaced by the even smaller krypton⁴⁵ or with methanol²³ or any other guest molecule, CA6 adopts the “round” form with all six O2(*n*)···O3(*n*−1) hydrogen bonds formed. Since the cavity is now too wide to provide a snug fit, the guest molecules are disordered, as in case of krypton and methanol.

2. Cooperative Networks Formed by O—H···O Hydrogen Bonds

Neutron diffraction was used to study form I of CA6·6H₂O so that all the hydrogen atoms could be located and the O—H···O hydrogen bonds could be determined. All the O—H hydrogen atoms are well ordered, and since so many O—H groups (18 from each CA6 and 12 from the 6 water molecules) occupy the crystal asymmetric unit, extended networks of O—H···O hydrogen bonds are formed. They are not organized at random but form “infinite” chains and circular structures with four, five, and six-membered rings predominating, where the O—H···O all point in the same direction, O—H···O—H···O—H··· This indicates the predominance of a cooperative effect⁴⁷ which, as shown by quantum chemical calculations, contributes about 25% of additional energy to the individual hydrogen bond.^{48,49} Since all the O—H groups point in the same direction, these patterns were called *homodromic*.⁴⁷ Besides these, *antidromic* arrangements are found in which one water molecule donates two hydrogen bonds in a chainlike or cyclic

motif which then collide on one oxygen acceptor. The *heterodromic* case with all O–H groups in random arrangement could not be identified, probably because it is less stable than the *homodromic* or *antidromic* forms.

3. Flip-Flop Hydrogen-Bond Disorder in CA7

Since CA7 has a wider cavity than CA6, it was not surprising to find that the hydrate CA7·12H₂O harbors seven water molecules in the molecular cavity. They are disordered over 11 partially occupied sites, and the remaining 5 water molecules are distributed over 8 sites located in interstices between the CA7 molecules. A neutron diffraction study with all CA7 and water O–H groups deuterated (O–D) showed that of the 53 O–D···O hydrogen bonds in the crystal asymmetric unit, 35 are of the type O–(¹/₂D)···(¹/₂D)–O, which was interpreted as dynamic equilibrium D–O···D–O ↔ O–D···O–D.^{50,51} These “flip-flop” hydrogen bonds are in fact due to a dynamical (and not static) disorder because CA7·12D₂O undergoes a reversible disorder–order phase transition at –46 °C as shown by calorimetric studies^{52,53} and a neutron diffraction analysis carried out at 120 K.⁵³ Quasi-elastic neutron scattering experiments^{55,56} have shown that the disorder is accompanied with jump rates (describing rotations of O–D groups) of up to $2 \times 10^{11} \text{ s}^{-1}$ at room temperature, in agreement with results obtained from molecular dynamics simulations.⁵⁷ The flip-flop disorder was found for all seven O2(*n*)···O3(*n*–1) interglucose hydrogen bonds in CA7 (Figure 8), and again in the deuterated complex CA7·ethanol·8D₂O.⁵⁸ This complex also shows a phase transition at around –50 °C, and crystal structure analyses of CA7·12D₂O and of CA7·ethanol·8D₂O at 120 K⁵⁴ and 15 K⁵⁹ respectively have shown that upon cooling, the flip-flop disorder of O–D groups and of water molecules has been replaced by strict order (except for a four-membered ring where flip-flop disorder remained). It comes as no surprise that the O–D···O–D···O–D hydroxyl groups are now aligned in the *homodromic* arrangement, indicating that the disordered O–D groups have oriented such that the energetic advantage due to cooperativity is optimized.

It should be stressed here that the flip-flop disorder of interglucose, intramolecular O2(*n*)···O3(*n*–1) hydrogen bonds appears to be a characteristic structural feature of CA7 and possibly also of CA8, but not of CA6. This is also consistent with the observation that X-ray analyses permitted the location of O2–H and O3–H hydrogen atoms only in CA6 crystal structures where they are fully ordered, whereas hydrogen atoms could not be located in CA7 and CA8, probably due to disorder. It appears that the flip-flop disorder is confined to CA with a ring size of seven and eight glucoses because the interglucose geometry is then optimal for the stabilization of O2(*n*)···O3(*n*–1) hydrogen bonds with three-center minor components to the glucosidic O4 (see section II.4 and Figure 5). This is supported by the observation (Table 1) that the O2(*n*)···O3(*n*–1) distances are in narrow ranges, 2.801–2.978 Å (average 2.884 Å)

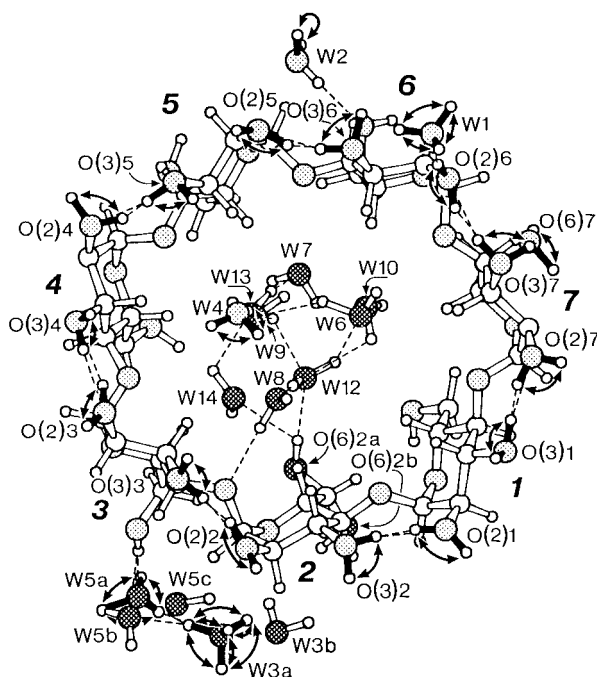


Figure 8. Section of the crystal structure of deuterated β -cyclodextrin (CA7)·12D₂O.⁵¹ All of the O2–D, O3–D hydroxyl groups (drawn with filled O–D bonds) show 2-fold flip-flop disorder indicated by curved double arrows; the distances between hydrogen atoms in O2···O3 hydrogen bonds are ~ 1 Å and too short to permit simultaneous, full occupation; consequently, these positions are only filled to about 50%. Oxygen atoms in light shading are fully occupied; in heavy shading, partially. Reprinted from ref 56. Copyright 1991 Taylor & Francis.

in CA7 and 2.765–2.911 Å (average 2.823 Å) in CA8, i.e., they are energetically similar. This contrasts with CA6 where O2(*n*)···O3(*n*–1) distances vary over a broader range, 2.902–3.150 Å (average 2.981 Å) and are considerably longer (and weaker) than in CA7 and CA8. Since the geometry in CA6 is different due to the increased curvature of the smaller ring, conditions for flip-flop disorder are apparently less suited than in CA7 and CA8. It should be noted that for entropic reasons, a flip-flop disorder network is more favored than a network with ordered O–H···O hydrogen bonds.

4. C–H···O Hydrogen Bonding Occurs if There Is a Lack of O–H Donors

The very detailed crystal structures of CA inclusion complexes have shown that besides normal O–H···O hydrogen bonding, there occur a large number of C–H···O hydrogen bonds that stabilize not only the host–guest interaction but they also contribute to the stabilization of the crystal lattice. A very good example of this interaction is shown in Figure 9 where hydroxyl groups from CA7, water, and ethanol and O(4) from CA7 are engaged as acceptors in C–H···O interactions. This suggests that an oxygen atom satisfies its acceptor hydrogen bonding potential with C–H hydrogens if not enough donor O–H hydrogen atoms are available;⁶⁰ in fact in carbohydrate crystal structures, 25% of the hydrogen bonds are of the C–H···O type.¹⁶

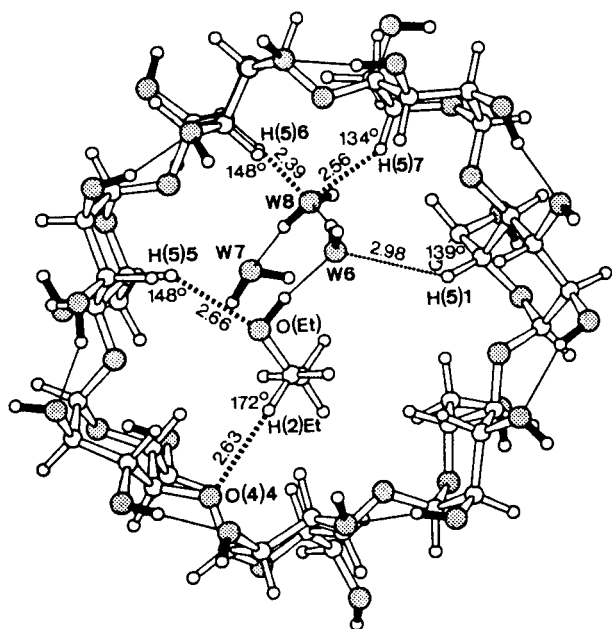


Figure 9. Hydrogen-bonding interactions of type O—D···O (thin lines) and C—H···O (dotted lines) in deuterated β -cyclodextrin (CA7) complexed with ethanol (EtOD) and 8 D₂O as obtained from a neutron diffraction study at 15 K. The cavity accommodates one ethanol and three water molecules W6, W7, and W8. Oxygen atoms shown dotted, O—D as filled bonds. Reprinted from ref 59. Copyright 1990 American Chemical Society.

In the glucose units of the CA, intramolecular C—H···O interactions are observed that contribute to the conformational stability. They are formed between C3—H(*n*), C5—H(*n*), and O4(*n*+1), and one of the two C6—H(*n*) hydrogen atoms is in close intraglucocontact with O4(*n*) and interglucose contact with O5(*n*−1), thereby stabilizing the (−)-gauche torsion angle O5—C5—C6—O6, see Figure 5.

V. Diffusion of Water Molecules in the Crystal Lattice of CA7·12H₂O

The flip-flop disorder described in section IV.3 changes at about −50 °C to order, associated with a phase transition measurable by calorimetric methods.^{52,53} This suggests that the disordered water molecules in the crystal lattice are mobile to some extent, and that the O—H groups of CA7 may rotate. Since the CA7 molecules are packed in the CA7·12H₂O crystal structure in cage-type herringbone arrangement, it was of interest to see whether movement of water molecules was confined only to the cavities (7 water molecules disordered over 11 sites) and interstices (5 water molecules disordered over 8 sites) separately or whether they would also move *between* the cavities and interstices.

This was studied by X-ray analyses on CA7·12H₂O exposed to different relative humidities (r.h.) in the range of 100% to 15%. The crystals did not decompose but their water content reduced continuously from 12 to 9.4 molecules per CA7 and the crystal unit cell volume shrank by 2.3%.⁶¹ At different r.h., X-ray structure analyses were carried out which clearly indicated that the water escapes preferentially the CA7 cavity and is more retained in the interstices between the CA7 molecule.⁶² This is probably as-

sociated with the more hydrophobic character of the cavity in relation to the more hydrophobic interstices containing most of the CA7 O—H groups.

Since it was of interest to determine the rate of water diffusion through the crystal lattice of CA7·12H₂O, a Raman spectroscopic study was carried out where powdered CA7·12H₂O crystals were exposed to D₂O atmosphere.⁶³ The H₂O/D₂O ratio in the sample was directly monitored using the Raman bands at 2300 and 3400 cm^{−1} characteristic of O—D and O—H stretching vibrations. The H₂O/D₂O exchange follows first-order kinetics $C_{\text{H}_2\text{O}} = C_{\text{H}_2\text{O},0}e^{-kt}$, with $C_{\text{H}_2\text{O},0}$ being the H₂O concentration at the beginning of the experiment and $k = 1.4 \times 10^{-2} \text{ min}^{-1}$, i.e., after 50 min, 50% of the H₂O is replaced by D₂O. The exchange is fully reversible so that H₂O can be replaced by D₂O and vice versa, and *all* the H₂O and O—H groups in CA are exchanged with D₂O and O—D, indicating that no O—H is engaged in such a strong hydrogen bond that it could not experience exchange with D. In a similar experiment, the dehydration/rehydration of CA7·12H₂O was measured, again finding first-order kinetics with a half-time of ~35 min.⁶⁴

The question remains whether D and H are transported by diffusion of *intact* water molecules or by chains of H⁺ (or D⁺) transfer processes, with OH[−] (or OD[−]) remaining at the surface. This question was tackled in a complementary experiment in which CA7·12H₂¹⁶O was exposed to an atmosphere of H₂¹⁸O and after defined time periods, samples were transferred to a mass spectrometer.⁶³ The kinetics of the ¹⁶O—¹⁸O exchange agreed with those of the H/D exchange reported above, and the analysis showed that, finally, *all* H₂¹⁶O were replaced by H₂¹⁸O, although there are no continuous channels in the CA7·12H₂O crystal lattice. This indicates that molecular and atomic movements occur in the crystal lattice of CA7·12H₂O which transiently open paths so that H₂O can diffuse; this is supported by molecular dynamics calculations indicating that atoms in CA7·12H₂O vibrate with amplitudes around 0.4 Å.⁶⁵ As estimated from the measured kinetics, the diffusion constant, $D \approx 3 \times 10^{-8} \text{ cm}^2 \text{ s}^{-1}$ is about 1/1000 that in pure water, $D \approx 2.2 \times 10^{-5} \text{ cm}^2 \text{ s}^{-1}$.

VI. CA9 Is the Intermediate between Smaller and Larger Cycloamyloses

CA9 is not commercially available as it is produced by the glucosyltransferases in only very small amounts and the purification is difficult. Therefore, only one crystal structure, that of CA9·13.75H₂O, has been published so far.⁶ It is of the herringbone cage type with most of the water molecules and some of the O6 hydroxyls of CA9 disordered. In contrast to CA6 to CA8, the macrocycle of CA9 is distorted such that the O4 atoms describe an ellipse shaped like a boat (Figure 10A,D). The O2,O3 hydroxyls are on the wider “deck” side and form hydrogen bonds with O2(*n*)···O3(*n*−1) distances varying much more than observed for CA6 to CA8, 2.741–3.234 Å, average 2.906 Å, see Table 1. In fact, there are even two diametrically opposed indentations suggesting that here the structure shows greatest distortion, whereas the other O2(*n*)···O3(*n*−1) hydrogen bonds are more

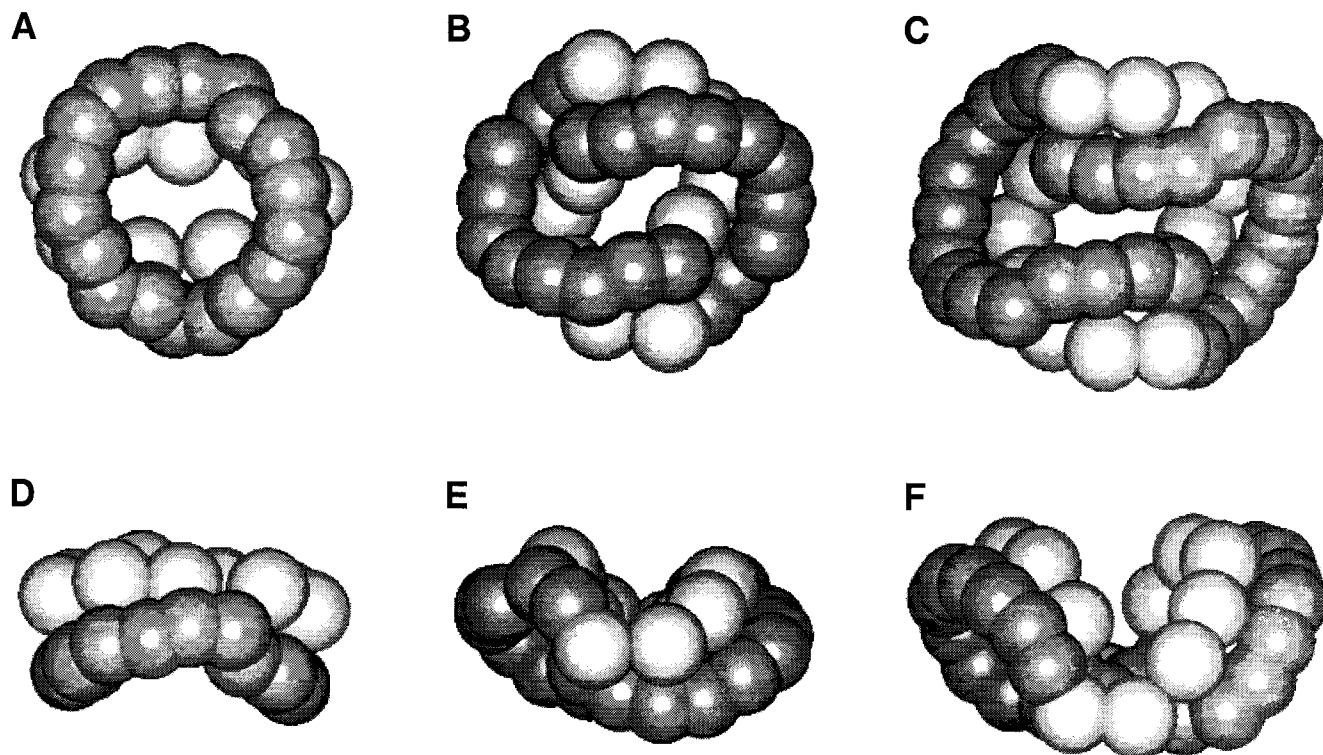


Figure 10. Schematic representation in top and side views of the molecular structures of CA9 (A, D), CA10 (B, E), and CA14 (C, F), to show the distortions associated with increase in ring size of the cycloamyloses. In Figures B, E, C, and F, the flips occur where the course of the O2, O3, and C6 atoms is broken. For clarity, only O2, O3 (dark) and C6 (light) atoms are drawn. For numbering of O2 and O3 hydroxyl groups, see Figure 4. Reprinted from ref 7. Copyright 1998 VCH Publishers.

“normal”. The O6 hydroxyls are at the narrower “hull” side of the boat-shaped molecule and point toward the central cavity, which is considerably collapsed compared with CA6 to CA8. As indicated by molecular modeling, the distorted boat-shaped structure of CA9 is enforced by steric strain resulting from the large ring size.⁷ It appears that CA9 has the maximum number of glucose residues for formation of an annular structure and that an increase by one or even more glucoses must result in a structure that deviates substantially from the doughnut shape that is characteristic for CA6 to CA8 (and still for CA9).

VII. Strain-Induced Flips of Glucoses and Kinks in Ca10 and Ca14

Recently, larger CAs with 100 and more glucoses in the ring became available by preparative-scale treatment of amylose with a disproportionating enzyme.¹⁰ ¹³C NMR studies⁷ showed that the structures of CA6 to CA8 are different from CA10 and its higher homologues, and X-ray structures identified a novel structural motif, the band flip, in CA10, CA14, and CA26.

1. ¹³C NMR Spectra Indicate Different Structures

¹³C NMR spectroscopy on the series formed by CA6 to CA26 showed only one sharp signal for each of the six glucose carbon atoms in the different CA, indicating that glucoses are identical on the NMR time scale.^{7,8} Increasing the ring size mainly affects ¹³C1 and ¹³C4 signals, while resonances of the other

carbons are only marginally influenced. For CA6 to CA8, ¹³C1 and ¹³C4 signals occur at ~102.4 and ~81.8 ppm respectively; for CA10 and the higher homologues, these signals shift to ~100.2 and ~78.3 ppm, suggesting some as yet undefined structural differences. The signals for CA9 are intermediate, ¹³C1 at 100.9 ppm and ¹³C4 at 79.2 ppm. The shift in ¹³C1 and ¹³C4 signals between CA8 to CA10 indicates clear distinction of two structural types; one is defined by CA6 to CA8 and the other by the higher homologues from CA10 on. However, according to its ¹³C signals, CA9 could occur in both forms, the observed singlets being indicative of rapid structural changes well below the millisecond NMR time scale.

2. CA10 and CA14 Are Not Doughnut-Shaped

The nature of the differences between the two structural forms of CA has been elucidated by X-ray analyses of CA10^{7,8} and CA14⁷ (ϵ - and ι -cyclodextrin or cyclodeca- and cyclotetradecaamylose) crystallized from aqueous solutions as 20.3 and 27.3 hydrates, respectively.⁷ Both crystals belong to the monoclinic space group C2 with half a molecule in the asymmetric unit, the second half being related to the first by crystallographic 2-fold rotation symmetry. The molecular shapes of CA10 and CA14 are very different compared to the shapes of the smaller CA6 to CA9 (Figure 10 parts B, E and C, F). This is due to the ~180° flipping of two diametrically opposed glucoses so that the ring of intramolecular O2(*n*)...O3(*n*-1) hydrogen bonds, which is still present in CA9, is disrupted. At the flip site, two adjacent glucoses are oriented trans, the other glucoses still

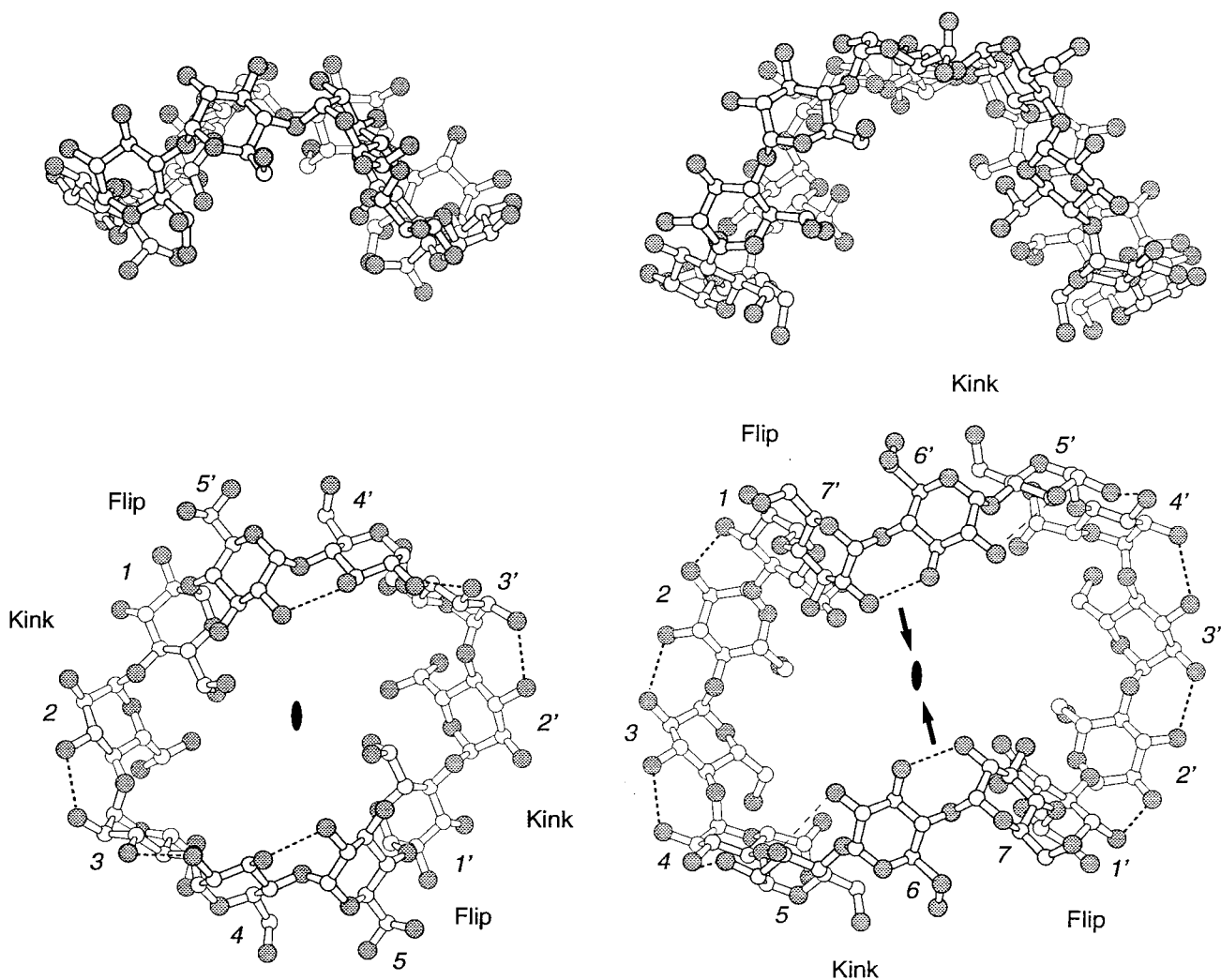


Figure 11. Molecular structures of CA10 (left) and CA14 (right) in top and side views, water omitted for clarity. The positions of the crystallographic 2-fold rotation axes are indicated (solid oval), glucoses in the two asymmetric units are denoted with primed and unprimed numbers. Oxygen and carbon atoms drawn as large (dotted) and small spheres, respectively; O6 oxygen atoms of glucoses 1, 2, 3, and 5 in CA10 and 1, 4, and 6 in CA14 are 2-fold disordered. Dotted lines suggest possible hydrogen bonds with O...O distances smaller than 3.5 Å, flip and kink are marked. In CA14, the thick arrows in the center indicate how glucoses might approach each other in larger cycloamyloses to form antiparallel double-helical structures with hydrogen bonds formed between O2 and O3 hydroxyl groups (see also Figure 13). Figures drawn with MOLSCRIPT.⁷⁷

remaining cis, but all are rotated. This is analogous to a band that is cut in two halves, on each half one of the end residues is rotated 180°, and the two halves are glued back together. For this reason, this new structural motif was called² “band flip”⁷ (Figure 11A,

B). As a consequence of these two symmetrically arranged “band flips”, the molecules are clearly divided into two halves connected at the flip sites. The central cavities are no longer open and round as in the smaller homologues but more slitlike, and the elliptically distorted molecules adopt molecular shapes resembling butterflies with the band flips located at the “body” and the wings formed by CD-like segments.

3. “Band Flips and Kinks as New Structural Features in CA Containing More than Nine Glucoses

There are significant conformational differences between CA10 and CA14. In CA10, the band-flip

occurs between glucoses G5' and G1 (primed and unprimed numbers refer to glucoses in one or the other symmetry related halves of CA10 and CA14). The orientation of flipped glucose G1 is stabilized by three-center hydrogen bonds¹⁶ donated by O3(5'), namely O3(5')...O6(1)B, 2.74 Å and O3(5')...O5(1), 3.21 Å (Figure 12A). Between the next two glucoses G1 and G2, a kink increases the O2(2)...O3(1) distance to 3.94 Å so that the hydrogen bond is broken; instead, a hydrogen bond unusual for oligosaccharides O6(1)A...O6(2)B, 3.08 Å, is formed between these two glucoses and may contribute to the stabilization of the kink; these two O6 hydroxyls point toward the cavity of CA10 and delimit its width (Figure 10A). The remaining glucoses (G2 to G5) are in the usual cyclodextrin-like arrangement with interglucose O2(*n*)...O3(*n*−1) hydrogen bonding distances in the range 2.89–3.03 Å.

In CA14, the flipped glucose G1 is again held in orientation by a three-center hydrogen bond donated

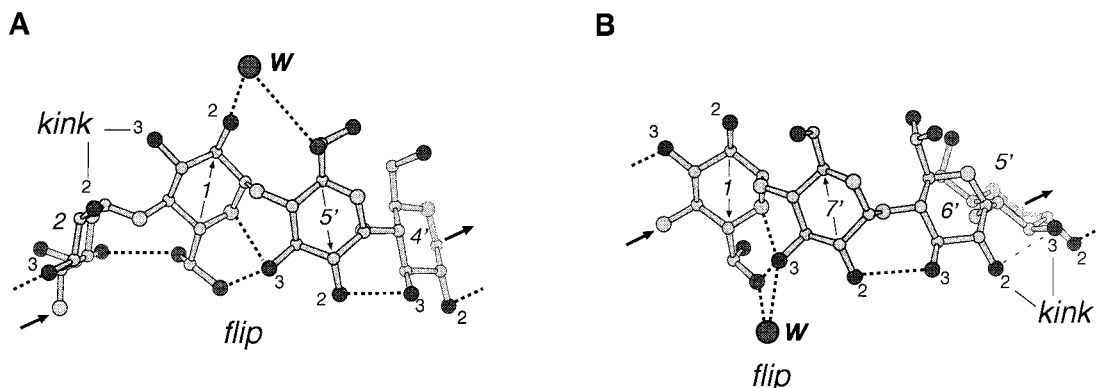


Figure 12. Structural details of kink and flip sites in CA10 (A) and CA14 (B). Water oxygens are shown as large spheres (labeled W); glucose oxygen and carbon atoms are drawn with large and small spheres, respectively; O2, O3, O6 darker; O2, O3 are numbered. View is from the center of the molecules. Note that the flips with trans oriented glucoses are stabilized by three-center hydrogen bonds $O(3)\cdots O(5')/O(6')$; in (+)gauche between glucoses 1 and 5' in CA10 (A) and between 1 and 7' in CA14 (B). The kink in CA10 is stabilized by an unusual hydrogen bond between O6 hydroxyls, $O6(1)A\cdots O6(2)B$, 3.06 Å. The $O2(1)\cdots O3(2)$ distance at this kink site is too long (3.94 Å) to be hydrogen bonded, whereas in CA14, the $O3(5)\cdots O2(6)$ distance of 3.40 Å is indicative of a long, weak hydrogen bond. The orientations of the glucoses at the flip sites are marked by arrows, and thick arrows at O4 and C1 atoms at both ends of the flip sites delineate the course of the CA chain. Reprinted from ref 7. Copyright 1998 VCH Publishers.

by $O3(7')$; namely $O3(7')\cdots O6(1)B$, 3.05 Å and $O3(7')\cdots O5(1)$, 3.32 Å; reminiscent of the geometry around the band-flip site in CA10 (Figure 12B). There is also a kink which, in contrast to CA10, does not directly follow the band-flip site but occurs between glucoses G5 and G6, and is stabilized by a long (weak) $O2(6)\cdots O3(5)$ hydrogen bond of 3.40 Å. All other $O2(n)\cdots O3(n-1)$ hydrogen bonds including those adjacent to the flip site are in the common range, 2.75 to 2.89 Å. In contrast to CA10, the narrowest diameter of the slitlike cavity in CA14 is formed by the O2, O3 hydroxyls of glucoses G6 and G7 preceding the band-flip site.

The band flip is best described by torsion angles ϕ and ψ .^{7,11} They are in the normal range for the $O2(n)\cdots O3(n-1)$ hydrogen bonded glucoses in the two halves, ϕ (94.1–102.1°); ψ (96.3°–122.0°) in CA10 and ϕ (96.6–110.2°); ψ (103.6–135.2°) in CA14 (Table 1). However for the flipped glucoses, these torsion angles are $\phi = 84^\circ$; $\psi = -65^\circ$ for G5–G1' in CA10 and $\phi = 82^\circ$; $\psi = -69^\circ$ for G7–G1' in CA14, and for the kinked glucoses $\phi = 76^\circ$, $\psi = 84^\circ$ in CA10 and $\phi = 93^\circ$; $\psi = 92^\circ$ in CA14.⁷ Despite these structural peculiarities, all glucoses in CA10 and CA14 are in 4C_1 conformation and unstrained as indicated by Cremer and Pople¹⁸ puckering parameters (not shown), by the virtual $O4(n)\cdots O4(n-1)$ distances (4.36–4.63 Å for CA10 and 4.45–4.61 Å for CA14) and by the angles subtended by O4 atoms, $O4(n)\cdots O4(n-1)\cdots O4(n-2)$, 126.7–145.9° for CA10 and 131.6–142.5° for CA14, Table 1.

The two band flips observed in CA10 and CA14 are a novel structural motif in (cyclo)amyloses and may occur whenever steric strain has to be relieved. They have comparable structure as indicated by ϕ and ψ torsion angles, and the trans orientations of adjacent glucoses are stabilized by $O6(n)B\cdots O3(n-1)$ and $O5(n)\cdots O3(n-1)$ hydrogen bonds. It appears that this motif, although less preferred, is as characteristic for amylose structures as the common motif where adjacent glucoses are in register (in cis) and $O2(n)\cdots O3(n-1)$ hydrogen bonded. If these two motifs do not

suffice in stabilizing an amylose structure in a low energy conformation, kinks are introduced. They can vary in degree and position along the amylose chain and are stabilized either by $O6(n)(+gauche)\cdots O6(n-1)(-gauche)$ or by long $O2(n)\cdots O3(n-1)$ hydrogen bonds as shown for CA10 and CA14, respectively.

4. Band Flips Must Occur Due to Conformational Strain

The energetics of the CA molecules, CA6 to CA10 and CA14, have been investigated by two complementary methods. First, the structures obtained from the X-ray study were energy minimized in a vacuum using the CHARMM22 force field. Second, the solvation energy was calculated using the Poisson–Boltzmann program SOLVATE.⁷ The sum of force field energy and solvation energy per glucose unit are remarkably similar for all molecules, ranging from –7.42 kcal/mol (CA6) to –7.94 kcal/mol (CA10). By contrast, the contributions of individual energy terms in that sum can vary significantly. This is especially true for the energetic changes in CA10 and CA14 in connection with the two band flips. There, due to the disturbed chain of intramolecular $O2(n)\cdots O3(n-1)$ hydrogen bonds, the Coulombic energy per glucose unit in CA10 is 2 kcal/mol higher than the corresponding energy in CA9. However, this difference is balanced by the more relaxed torsion angle energies and the better solvation of CA10.

5. Extension of the Structure of CA10 and CA14 to Very Large CA—A Plausible Model

One could assume that all very large CAs will exhibit comparable structures. This is because in CA14, the band-flip site forms short $O2(n)\cdots O3(n-1)$ hydrogen bonds to preceding and following glucoses. Additional glucoses in larger CA may be added at the band-flip sites to form strings of $O2(n)\cdots O3(n-1)$ hydrogen bonded glucoses, and the kink may vary (and even disappear), depending on residual strain energy. The two strings in opposite

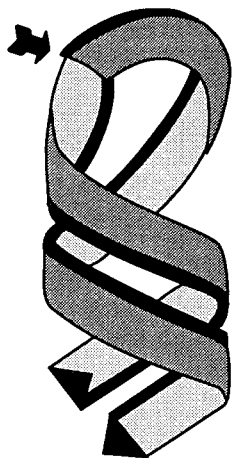


Figure 13. Illustration of the proposed antiparallel left-handed, double helical form (only half a molecule) for larger cycloamyloses. The O2, O3 chain of the molecule is indicated by the solid line. It is interrupted at the flip site marked by the arrow. Reprinted from ref 7. Copyright 1998 VCH Publishers.

orientation may approach each other and associate across the center of the molecule through hydrogen bonds between O2 and O3 hydroxyl groups (see caption to arrow in Figure 11B). Since the strings will be twisted in cyclodextrin-like form due to their $O2(n) \cdots O3(n-1)$ hydrogen bonding, we anticipate formation of a left-handed antiparallel double helix (Figure 13) as observed in the crystal structure of (*p*-nitrophenyl- α -maltohexaoside) $_2 \cdot Ba(I_3)_2 \cdot 27H_2O$.^{66–68}

6. CA10 and CA14 in Solution—Do They Form Inclusion Complexes?

The three-dimensional structures of CA10 and CA14 appear to be relatively rigid even in solution because these molecules crystallize as readily as the smaller cyclodextrins, in contrast to linear maltooligomers with their high degrees of conformational freedom. The three-dimensional structures of CA10 and CA14 are not only stabilized by intramolecular, interglucose hydrogen bonding but also by interactions with water molecules in hydrogen bonding contacts with the glucose hydroxyl groups (not shown). The water molecules are mostly disordered and located in the narrow cavities enclosed between the rows of O2, O3 groups on one side and of O6 groups on the other (Figure 10C–F). In solution, CA10 and CA14 undergo conformational changes that are fast on the NMR time scale as all CAs show only six ^{13}C signals and no doublets for C1 and C4. We assume that the chain flips move along the chains and/or glucoses flip back to form much distorted cyclodextrin-like structures.

It is not yet clear whether the larger cycloamyloses CA10 and beyond will form inclusion complexes as observed for the cyclodextrins, CA6 to CA8. A preliminary note⁸ reports the structure of CA10 crystallized from a 1:1 mixture of water and acetonitrile. The crystals, however, are identical to those obtained from pure water⁷ and had not formed a complex with the organic solvent. This suggests that the inclusion properties of CA10 are different to the cyclodextrins CA6 to CA8 which may accommodate

many kinds of guest molecules, among them acetonitrile,⁶⁹ in their central, round cavities, permitting a snug fit. In CA10 and the higher homologues, a guest molecule would not experience a comparably close proximity to the host molecules, because their cavities are so distorted into narrow grooves that only guest molecules with geometries complementary to these grooves might be able to form inclusion complexes. This could open avenues for very specific host–guest interactions with the larger CA molecules.

On the other hand, the situation may be different with CAs large enough to form an antiparallel double helix as proposed above (Figure 13). The double helix contains a central, channel-like cavity which may accommodate guest molecules of suitable size, analogous to the inclusion of ployiodide $(I_3^-)_n$ in the double helix formed by (*p*-nitrophenyl- α -maltohexaoside) $_2 \cdot Ba(I_3)_2 \cdot 27H_2O$.^{66,67} This view is supported by the observation (unpublished) that CA50 and larger show properties similar to linear amylose. They form precipitates from aqueous solutions if higher alcohols or long fatty acids are added, and produce blue or brown complexes with iodine depending on their size. This could, however, be due to inclusion into the channel-like cavities in helices of the V-amylose type as shown below.

VIII. A Glimpse at the Structure of CA26—Déjà Vu Cyclodextrin and Band Flips: The V-Amylose Helix

The crystal structure of CA26 hydrate⁹ contains $(CA26)_2 \cdot 78H_2O$ in the triclinic unit cell. It shows that the CA chain is not folded as proposed on the basis of the structure of CA14 (Figure 14) with central antiparallel, left-handed double helix and two band flips in the loops. By contrast, CA26 adopts the shape of a figure eight in which each half consists of two left-handed, single helical turns with six glucoses per repeat, the same conformation as proposed for V-amylose on the basis of X-ray fiber and electron diffraction,^{70–72} and ^{13}C –CP MAS NMR.^{73,74} The turns are stabilized by hydrogen bonds formed internally between the glucoses $O2(n) \cdots O3(n-1)$, and between the turns by O2 and O3 \cdots O6. At the “upper” and “lower” sides, the short helices are connected by two stretches of three glucoses containing one band flip each. The flips have geometries as described for CA10 and CA14 in Figure 12, i.e., the structure of CA26 hydrate is modular with elements taken from CA6 and CA10 and from V-amylose.

The two short single helices in CA26 contain channel-like cavities with a similar width as found in α -cyclodextrin. They accommodate disordered water molecules but could also enclose other molecules of suitable size. Such inclusion complexes have actually been observed for very long CA (see above).

The amylose chain in CA26 hydrate is folded such that the two single helical structures in the figure eight are tightly associated though hydrogen bonding and van der Waals interactions. It appears that this structural organization is very specific for a CA of

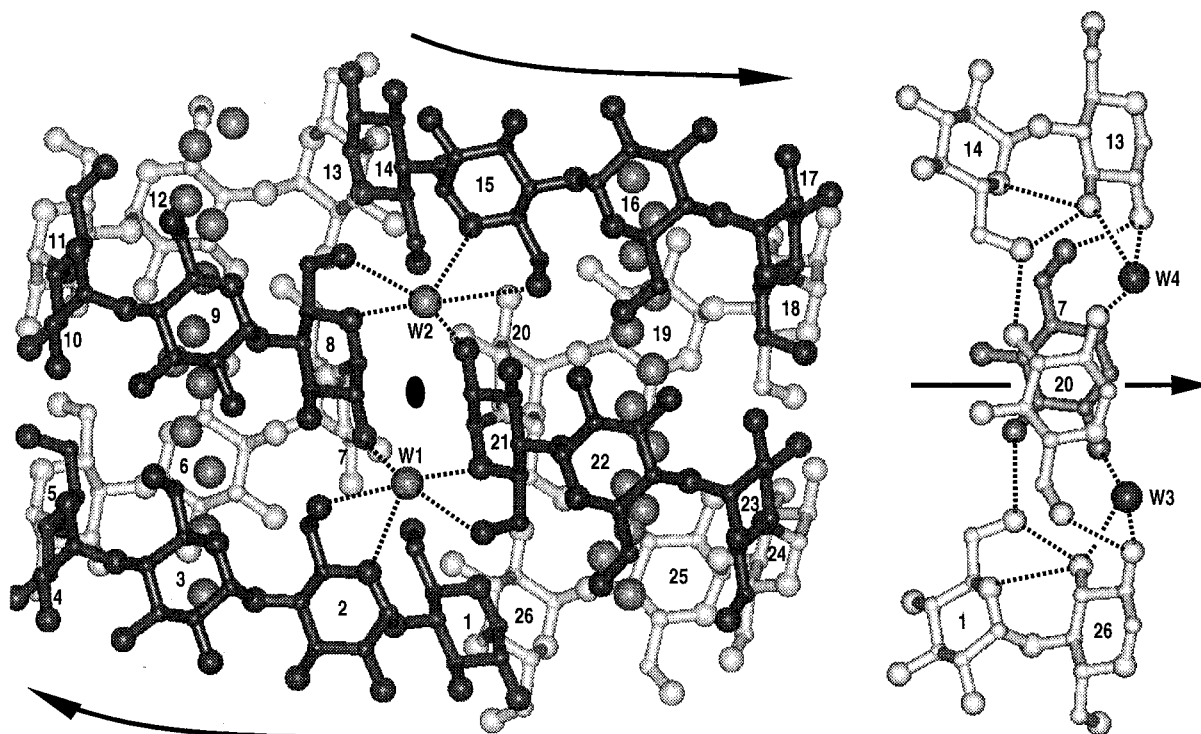


Figure 14. (Left) Folding of the CA chain in CA26 shows pseudo-2-fold rotation symmetry with the axis vertical to the plane of the paper at the solid oval. Glucoses are numbered 1 to 26, parts in the front are darker than those in the back. Band flips occur between glucoses 13,14 and 26,1: the arrows indicate left-helical V-amylose turns with six glucoses per pitch. Hydrogen bonds are shown only for water coordination; all others are omitted for clarity. Water molecules W1, W2 and W3, W4 (not shown in this drawing) stabilize the folding. (Right) Section of the structure showing band flips linked by hydrogen bonding to water molecules W3, W4 and to glucoses G7, G20 which form the interface between the two V-helices. Taken from ref 9.

this particular size. If the length of the amylose chain is extended or shortened by only few glucose units, the tight intramolecular packing will be changed adversely so that structural reorganization might occur. This view is supported by the finding that we were able so far to crystallize only CA10, CA14, and CA26 although we have available the whole series of CAs. It could well be that the figure eight shape of CA hydrate is only one possible molecular structure of long CA, and others are provided by the folding with central antiparallel double helix as suggested in Figure 13. In fact, even other structures might be feasible, depending on the length of the CA chain, as illustrated by modeling of CA21 into different shapes that were used to interpret small-angle X-ray scattering data obtained for CA21 dissolved in water.⁷⁵

IX. Outlook

Although CAs have been known since 1903 when they were discovered by Schardinger,⁷⁶ they still provide surprises in research and applications. The most common members of this family of compounds, CA6 and CA7, play increasing roles in chemical and pharmaceutical industry, and they have been and still are utilized in model studies relating to noncovalent intermolecular interactions. In addition, they belong to the best known "supramolecular compounds" and consequently are of current interest also in relation to other synthetically prepared ring-shaped molecules. The very recent emergence in

preparative quantities of the very long CAs has widened the horizon of the CAs considerably. With the structure determinations, their geometrical properties and characteristics have been described—their solution and inclusion properties have yet to be elucidated, not to mention the possible industrial applications.

X. Acknowledgments

The continuing financial support of the structural studies described here by Deutsche Forschungsgemeinschaft, Fonds der Chemischen Industrie and Bundesministerium für Forschung und Technologie is gratefully acknowledged.

XI. References

- (1) Szejtli, J. *Cyclodextrin Technology*; Kluwer Academic Publishers: Dordrecht, 1988.
- (2) Duchêne, D., Ed. *Cyclodextrin and their Industrial Uses*; Editions de Santé: Paris, 1987.
- (3) Saenger, W. *Angew. Chem., Int. Ed. Engl.* **1980**, *19*, 344.
- (4) Saenger, W. In *Inclusion Compounds*; Atwood, J. L., Davies, J. E. D., MacNicol, D. D., Eds.; Academic Press: London, 1984; Vol. 2, pp 231–260.
- (5) Harata, K. In *Inclusion Compounds*; Atwood, J. L., Davies, J. E. D., MacNicol, D. D., Eds.; Academic Press: London, 1991; Vol. 5, p 311.
- (6) Fujiwara, T.; Tanaka, N.; Kobayashi, S. *Chem. Lett.* **1990**, 739.
- (7) Jacob, J.; Gessler, K.; Hoffmann, D.; Sanbe, H.; Koizumi, K.; Smith, S. M.; Takaha, T.; Saenger, W. *Angew. Chem., Int. Ed. Engl.* **1998**, *37*, 606.
- (8) Ueda, H.; Endo, T.; Nagase, H.; Kobayashi, S.; Nagai, T. *J. Inclusion Phenom. Mol. Recognit. Chem.* **1996**, *25*, 17.

- (9) Gessler, K.; Uson, I.; Takaha, T.; Krauss, N.; Smith, S. M.; Okada, S.; Sheldrick, G. M.; Saenger, W. Submitted for publication.
- (10) Takaha, T.; Yanase, M.; Takata, S.; Okada, S.; Smith, S. M. *J. Biol. Chem.* **1996**, *271*, 2902.
- (11) Definition of ϕ , ψ torsion angles: ϕ , O5(*n*)–C1(*n*)–O4(*n*–1)–C4(*n*–1); ψ , C1(*n*)–O4(*n*–1)–C4(*n*–1)–C3(*n*–1), see IUPAC Rules: *Eur. J. Biochem.* **1983**, *131*, 5.
- (12) Cramer, F. *Einschlussverbindungen*; Springer-Verlag: Heidelberg, 1954.
- (13) Harata, K. In *Cyclodextrins. Comprehensive Supramolecular Chemistry*; Atwood, J. L., Davies, J. E. D., MacNicol, D. D., Eds.; Pergamon: Oxford 1996, Vol. 3, Chapter 9.
- (14) Frömmling, K. H.; Szejtli, J. *Cyclodextrin in Pharmacy*; Kluwer Academic Publishers: Dordrecht 1994.
- (15) Wenz, G. *Angew. Chem., Int. Ed. Engl.* **1994**, *33*, 803.
- (16) Jeffrey, G. A.; Saenger, W. *Hydrogen Bonding in Biological Structures*; Springer-Verlag: Heidelberg, 1991; p 309.
- (17) Szejtli, J. *Cyclodextrin Technology*; Kluwer Academic Publishers: Dordrecht, 1988; p 48.
- (18) Cremer, C.; Pople, J. A. *J. Am. Chem. Soc.* **1975**, *97*, 1354.
- (19) Harata, K.; Hirayama, F.; Arima, H.; Mekama, K.; Miyaji, T. *J. Chem. Soc., Perkin Trans. 2* **1992**, 1159.
- (20) Caira, M. R.; Griffith, V. J.; Nassimbeni, L. R.; van Oudtshoorn, B. *J. Chem. Soc., Perkin Trans. 2* **1994**, 2071.
- (21) Bruck, T. K.; Weinhold, F. *J. Am. Chem. Soc.* **1979**, *101*, 1700.
- (22) Perez, S.; St.-Pierre, J.; Marchessault, R. H. *Can. J. Chem.* **1978**, *56*, 2866.
- (23) Hingerty, B.; Saenger, W. *J. Am. Chem. Soc.* **1976**, *98*, 3357.
- (24) French, A. D.; Murphy, V. G. *Carbohydr. Res.* **1973**, *27*, 391.
- (25) Pensak, D. A.; French, A. D. *Carbohydr. Res.* **1980**, *87*, 1.
- (26) Harata, K. *Bull. Chem. Soc. Jpn.* **1977**, *50*, 1416.
- (27) Casu, B.; Reggiani, M.; Gallo, G. G.; Vigevani, A. *Chem. Soc., Spec. Publ.* **1968**, *23*, 217.
- (28) Bergeron, R.; Channing, M. A. *Bioorg. Chem.* **1976**, *5*, 437.
- (29) Steiner, T.; Saenger, W. *Carbohydr. Lett.* **1994**, *1*, 143.
- (30) Harata, K.; Uekama, K.; Otagiri, M.; Hirayama, F.; Ogino, H. *Bull. Chem. Soc. Jpn.* **1981**, *54*, 1954.
- (31) Steiner, T.; Saenger, W. *J. Am. Chem. Soc.* **1992**, *114*, 10146.
- (32) Saenger, W. *Israel J. Chem.* **1985**, *25*, 43.
- (33) Lindner, K.; Saenger, W. *Biochem. Biophys. Res. Commun.* **1980**, *92*, 933.
- (34) Saenger, W.; Beyer, K.; Manor, P. C. *Acta Crystallogr. Sect. B.* **1976**, *32*, 120.
- (35) Harata, K. *Bull. Chem. Soc. Jpn.* **1978**, *51*, 1644.
- (36) McMullan, R. K.; Saenger, W.; Fayos, J.; Mootz, D. *Carbohydr. Res.* **1973**, *31*, 37.
- (37) Hybl, A.; Rundle, R. E.; Williams, D. E. *J. Am. Chem. Soc.* **1965**, *87*, 2779.
- (38) Harata, K. *Bull. Chem. Soc. Jpn.* **1987**, *60*, 2763.
- (39) Ding, J.; Steiner, T.; Zabel, C.; Hingerty, B. E.; Mason, S. A.; Saenger, W. *J. Am. Chem. Soc.* **1991**, *113*, 8081.
- (40) Steiner, T.; Saenger, W. *Acta Crystallogr. Sect. B*, in press.
- (41) Noltemeyer, M.; Saenger, W. *Nature* **1976**, *259*, 629; *J. Am. Chem. Soc.* **1980**, *102*, 2710.
- (42) Manor, P. C.; Saenger, W. *Nature* **1972**, *237*, 392; *J. Am. Chem. Soc.* **1974**, *96*, 3630.
- (43) Lindner, K.; Saenger, W. *Acta Crystallogr. Sect. B* **1982**, *38*, 203.
- (44) Chacko, K. K.; Saenger, W. *J. Am. Chem. Soc.* **1981**, *103*, 1708.
- (45) Saenger, W.; Noltemeyer, M. *Chem. Ber.* **1976**, *109*, 503.
- (46) Klar, B.; Hingerty, B.; Saenger, W. *Acta Crystallogr. Section B* **1980**, *36*, 1154.
- (47) Saenger, W. *Nature* **1979**, *279*, 343.
- (48) Lesyng, B.; Saenger, W. *Biochim. Biophys. Acta* **1981**, *678*, 408.
- (49) Koehler, J. E. H.; Saenger, W.; Lesyng, G. *J. Comput. Chem.* **1987**, *8*, 1090.
- (50) Saenger, W.; Betzel, Ch.; Hingerty, B.; Brown, G. M. *Nature* **1982**, *296*, 581.
- (51) Betzel, Ch.; Saenger, W.; Hingerty, B.; Brown, G. M. *J. Am. Chem. Soc.* **1984**, *106*, 7545.
- (52) Fujiwara, T.; Yamazaki, Y.; Tomizu, R.; Tokuoka, R.; Tomita, K.-I.; Matsuo, T.; Suga, H.; Saenger, W. *Chem. Soc. Jpn. (Nippon Kagaku Kaishi)* **1983**, 181.
- (53) Hanabata, H.; Matsuo, T.; Suga, H. *J. Inclusion Phenom.* **1987**, *5*, 325.
- (54) Zabel, V.; Saenger, W.; Mason, S. A. *J. Am. Chem. Soc.* **1986**, *108*, 3664.
- (55) Steiner, T.; Saenger, W.; Kearley, G.; Lechner, R. E. *Physica B* **1989**, *156/157*, 336.
- (56) Steiner, T.; Saenger, W.; Lechner, R. E. *Mol. Phys.* **1991**, *72*, 1211.
- (57) Koehler, J. E. H.; Saenger, W.; van Gunsteren, W. F. *Eur. Biophys. J.* **1987**, *15*, 211.
- (58) Steiner, T.; Mason, S. A.; Saenger, W. *J. Am. Chem. Soc.* **1991**, *113*, 5676.
- (59) Steiner, T.; Mason, S. A.; Saenger, W. *J. Am. Chem. Soc.* **1990**, *112*, 8164.
- (60) Steiner, T. *Crystallogr. Rev.* **1996**, *6*, 1; *Chem. Commun.* **1997**, 727.
- (61) Steiner, T.; Koellner, G.; Ali, S.; Zakim, D.; Saenger, W. *Biochem. Biophys. Res. Commun.* **1992**, *188*, 1060.
- (62) Steiner, T.; Koellner, G. *J. Am. Chem. Soc.* **1994**, *116*, 5122.
- (63) Steiner, T.; Moreira da Silva, A. M.; Teixeira-Dias, J. J. C.; Müller, J.; Saenger, W. *Angew. Chem., Int. Ed. Engl.* **1995**, *34*, 1452.
- (64) Moreira da Silva, A. M.; Steiner, T.; Saenger, W.; Empis, J.; Teixeira-Dias, J. J. C. *Chem. Commun.* **1996**, 1871.
- (65) Koehler, J. E. H.; Saenger, W.; van Gunsteren, W. F. *Eur. Biophys. J.* **1988**, *16*, 153.
- (66) Hinrichs, W.; Büttner, G.; Steifa, M.; Betzel, Ch.; Zabel, V.; Pfannemüller, B.; Saenger, W. *Science* **1987**, *238*, 205.
- (67) Hinrichs, W.; Saenger, W. *J. Am. Chem. Soc.* **1990**, *112*, 2789.
- (68) Schulz, W.; Sklenar, H.; Hinrichs, W.; Saenger, W. *Biopolymers* **1993**, *33*, 363.
- (69) Aree, T.; Jacob, J.; Saenger, W.; Hoier, H. *Carbohydr. Res.*, in press.
- (70) Sarko, A.; Zugenmaier, P. In *Fiber Diffraction Methods*; French, A. D., Gardner, K. C. H., Eds.; ACS Sympos. Series No. 141; American Chemical Society: Washington, DC, 1980.
- (71) Rappenecker, G.; Zugenmaier, P. *Carbohydr. Res.* **1981**, *89*, 11.
- (72) Brisson, J.; Chanzy, H.; Winter, W. T. *Int. J. Biol. Macromol.* **1991**, *13*, 31.
- (73) Veregin, R. P.; Fyfe, C. A.; Marchessault, R. H. *Macromolecules* **1988**, *20*, 3007.
- (74) Gidley, M. J.; Bociek, S. M. *J. Am. Chem. Soc.* **1988**, *110*, 3820.
- (75) Kitamura, S.; Isuda, H.; Shimada, J.; Takada, T.; Takaha, T.; Okada, S.; Mimura, M.; Kajiwar, K. *Carbohydr. Res.* **1997**, *304*, 303.
- (76) Schardinger, F. *Z. Nahr. u. Genussm.* **1903**, *6*, 865.
- (77) Kraulis, P. J. *J. Appl. Crystallogr.* **1991**, *24*, 946.

CR9700181